UDK 531.226:552.523
Original scientific article/Izvirni znanstveni članek

ISSN 1580-2949
MTAEC9, 56(1)39(2022)

EFFECTS OF INITIAL SHEAR STRESS AND VIBRATION FREQUENCY ON THE DYNAMIC STRENGTH CHARACTERISTICS OF SATURATED CLAY

VPLIV ZAČETNE STRIŽNE NAPETOSTI IN VIBRACIJSKE FREKVENCE NA KARAKTERISTIKE DINAMIČNE TRDNOSTI NASIČENE GLINE

Jian Zhang[1*], Yangguang Sun[2], Jiuting Cao[3], Baocun Shi[4]

[1]Nanjing Vocational Institute of Transport Technology, Nanjing 211188, China
[2]Guangdong Province Communications Planning and Design Institute Co.Ltd, Guangzhou 510507, China
[3]Jiangsu Zhongshe Group Co., Ltd., Wuxi 214072, China
[4]Hohai University, Nanjing 210098, China

Prejem rokopisa – received: 2021-11-12; sprejem za objavo – accepted for publication: 2021-12-11

doi:10.17222/mit.2021.315

Initial shear stress is inevitable in actual engineering slopes, subgrades and foundations. The soils exhibit different dynamic characteristics under an initial shear stress. The dynamic strength characteristics of saturated clay under cyclic loading were studied through a dynamic triaxial test of remoulded clay in the Wenchuan area. The effects of the failure criterion, initial shear stress and vibration frequency on the dynamic strength characteristics of saturated clay were also analysed. The results showed that the strain failure criterion with a strain value of 2.5 % or the transitional strain ε_{tp} can reflect the soil damage realistically and evaluate the dynamic strength of the soil objectively. $\varepsilon_p = 2.5$ % can be used to replace $\varepsilon_p = \varepsilon_{tp}$ when the dynamic strength parameter of the saturated clay was calculated under seismic loading equivalent failure vibration times. The dynamic strength parameters of the saturated clay under different earthquake magnitudes were calculated by introducing the equivalent failure vibration times of the soil under seismic loading, thereby providing data support for the stability analysis of the clay foundation under seismic loading. The initial shear stress and vibration frequency have a considerable effect on the dynamic strength of saturated clay. Under the same vibration frequency, the larger the initial shear stress is, the smaller the required dynamic stress is for the soil to break, and the smaller the dynamic strength parameter is. The existence of the initial shear stress reduces the dynamic strength of the soil. Under the same vibration times, the higher the vibration frequency is, the greater the required dynamic stress is for the soil to break, the larger the dynamic strength parameter is, and the greater the dynamic strength of the soil is.

Keywords: initial shear stress, saturated clay, dynamic strength parameter, failure criterion

Z začetno strižno napetostjo se neizogibno srečamo, ko obravnavamo probleme vezane na inženirske zemljine, hribine, strmine, nagibe, podzemelja, temelje itd. Vsi ti objekti različno dinamično reagirajo na prisotno začetno strižno napetost. Avtorji tega članka so analizirali obnašanje nasičene gline pod vplivom dinamičnih obremenitev. Za to so uporabili sistem za dinamično obremenilno triosno testiranje in v študiji raziskovali dinamično trdnost preoblikovane gline iz Wenchuana, provinca Sichuan na Kitajskem (potres 2008). Prav tako so analizirali vpliv kriterija porušitve, začetne strižne napetosti in vibracijske frekvence na dinamično trdnost preiskovane gline. Rezultati analiz so pokazali, da kriterij deformacijske porušitve pri deformaciji 2,5 % ali prehodni deformaciji ε_{tp} lahko realistično prikaže situacijo pri kateri pride do poškodb oz. porušitve in s tem objektivno ovrednoti dinamično trdnost tal oz. realne zemljine. Prehodno deformacijo $\varepsilon_p = 2{,}5$ % lahko uporabimo kot zamenjavo za $\varepsilon_p = \varepsilon_{tp}$, ko parameter dinamične trdnosti nasičene gline izračunamo pri enakih potresnih obremenitvah in z ekvivalentnimi vibracijskimi frekvencami potrebnimi za porušitev. Avtorji tega članka so izračunali parametre dinamične trdnosti nasičene gline pri različnih magnitudah potresov z uvedbo ekvivalentnih porušnih vibracijskih časov za dane potresne obremenitve. Na ta način so avtorji zagotovili podatkovno podporo za analizo stabilnosti temeljenja glinene podlage v primeru potresnih obremenitev. Začetna strižna napetost in vibracijska frekvenca imata pomemben vpliv na dinamično trdnost nasičene gline. Večja kot je začetna strižna napetost pri enaki vibracijski frekvenci, manjša je zahtevana dinamična napetost za porušitev zemljine in manjši je parameter dinamične trdnosti. Obstoj neke začetne strižne napetosti v zemljini zmanjša njeno dinamično trdnost. Večja kot je vibracijska frekvenca pri enakih vibracijskih časih, večja je zahtevana dinamična napetost za porušitev zemljine, večji je tudi njen parameter dinamične trdnosti in večja je njena dinamična trdnost.

Ključne besede: začetna strižna napetost, nasičena glina, parameter dinamične trdnosti, kriterij odpovedi (porušitve)

1 INTRODUCTION

China is an earthquake-prone country with a wide distribution of earthquakes. The earthquakes in its southwestern part are particularly strong. In the past 100 years, the number of strong earthquakes ($M = 8$) in China has been 10, and the casualties and property losses are severe in densely populated areas.[1–3] In 1920, the number of deaths in the Haiyuan earthquake in Ningxia was more than 200,000, and the wounded were innumerable. In 1976, a 7.8-magnitude earthquake struck Tangshan, Hebei Province. Most of the urban houses collapsed, more than 240,000 people suffered, and the wounded were countless. In 2008, Wenchuan, Sichuan Province, suffered an 8.0-magnitude earthquake with a maximum intensity of 11 degrees. The earthquake cov-

*Corresponding author's e-mail:
beifangnanhai19@163.com (Jian Zhang)

ered 10 provinces and cities; its destructiveness and difficulty of relief were quite rare, during which more than 80,000 people were dead or missing, causing major casualties and property losses.[4,5]

Earthquakes cause many foundations and subgrades to be liquefied, deformed and destroyed. For an earthquake-prone country like China, many foundations and roadbeds of buildings are likely to encounter earthquakes. In addition, many infrastructures are built on widely distributed soft clay foundations; the initial shear stress is inevitable in these foundations and roadbeds, and soft clay may exhibit different dynamic characteristics under the initial shear stress. Thus, the dynamic strength characteristics of soft clay under the initial shear stress must be studied, and the research results have a strong application value.[6–10]

At present, most of the tests mainly consider the state where the initial shear stress does not exist, i.e., the test is started based on the equal, three-dimensional consolidation pressure. The initial shear stress is an important factor affecting the dynamic properties of saturated clay, and many researchers are beginning to pay attention to study the effect of the initial shear stress. Yasuhara et al.[11] considered that under cyclic loading, the pore-water pressure inside the normally consolidated clay soil gradually increases with vibration times, decreasing the effective stress and dynamic strength of the soil. Moreover, the greater the residual pore pressure is, the higher the attenuation of the soil dynamic strength is. Ishihara et al.[12] showed that the existence of the initial shear stress increases the overall soil strength. Seed et al.[13], Zimmie et al.[14] and Goulois et al.[15] believed that the shear strength of soil gradually decreases with the increase of initial shear stress. Lefebvre et al.[16] determined through experiments that when the initial shear stress exists in the soil, the shear strength is reduced, while improving the total strength of the soil. Tan et al.[17] believed that the dynamic strength of clay gradually decreases with the increase of initial shear stress. Matisui et al.[18] found through clay cycle triaxial test that the shear strength of the soil is reduced when the cyclic stress is relatively large. Liao et al.[19] considered that the consolidation ratio has a considerable effect on the dynamic shear strength of volcanic ash clay soil through a dynamic triaxial test of volcanic ash clay soil. They also established a dynamic shear-strength expression for the consolidation ratio change. Chen et al.[20] determined by studying the cyclic loading that under the same dynamic stress level, the higher the vibration frequency is, the higher the dynamic strength of the soil is. The natural structure of the soil determines the difference in the dynamic strength of the soil at different frequencies. Moreover, frequency has a considerable influence on the dynamic strength, even if the vibration times are long.

The above analysis indicates that many infrastructures are built on widely distributed, soft clay foundations, and the initial shear stress is inevitable on these foundations. However, the influence of the initial shear stress and the vibration frequency on the dynamic strength characteristics of saturated clay has not been consistently concluded, and the relationship between the dynamic strength and the vibration times under different initial shear stresses has not been established. The dynamic strength of saturated clay is closely related to the selection of a failure criterion. At present, the selection of a failure criterion is not clear, and the variation law of strength parameters (c, φ) for soft clay under different magnitudes is not presented. Therefore, an experimental study of the dynamic strength characteristics of saturated clay, which provides a theoretical basis for the stability analysis of clay foundation under seismic loading, must be continued.

2 SOIL SAMPLES AND PLANS

2.1 Soil samples

The clay used in the experiment, which was reshaped, was taken from Wenchuan, Sichuan Province. The sampling depth was approximately 4–6 m. The basic physical properties of the clay are shown in **Table 1**. According to the classification criteria for clay soil, the clay in Wenchuan earthquake area was classified by plastic map, and the clay used in the test was viscous low plastic soil.

2.2 Test procedures and methods

This test used a triaxial apparatus (DDS-70, China). A remoulded soil sample with a diameter of 39.1 mm and a height of 80 mm was used. It was prepared using a multilayer wet-mortar method and divided into five layers for compaction. The weight of each layer was determined based on the dry density of the soil sample and the predesigned moisture content. Each layer was compacted to the corresponding height, and the contact surfaces were shaved to ensure good contact between the layers. After the sample preparation, the soil sample was installed in the pressure chamber of the cyclic triaxial apparatus. In the pressure chamber, two methods were used to saturate the sample, i.e., vacuum pumping, airless water and reversing pressure. When the pore-water pressure coefficient B was 0.97, the sample was considered to meet the saturation requirement. In the consolidation phase, the drain valve was opened slowly after the sam-

Table 1: Basic physical properties of clay

Density (g/cm^3)	Natural moisture content (w/%)	Proportion Gs	Liquid limit (w_L/%)	Plastic limit (w_P/%)	Plasticity index I_p	Cohesion (kPa)	Internal friction angle (°)
1.78	21.59	2.72	37.62	20.26	17.36	27.15	16.86

ple was saturated. The drain valve needed to be closed for 5 min when the pore-water pressure dissipated close to 0. The consolidation was considered complete when the pore-water pressure no longer increased. The deviatoric stress was gradually increased after the isostatic consolidation was completed. At this time, the drain valve needed to be opened to avoid deformation and damage. It was consolidated for pore-water pressure no longer increasing when applied to the corresponding deviatoric stress. Then, the drain valve was closed to complete the bias-consolidation process.

2.3 Test plans

According to the depth of the soil extraction and research needs, the consolidation confining pressures in this test are σ_c (50; 100; 150) kPa. Given the short acting time of the cyclic loading provided by the earthquake, the drainage of the clay layer is slow. The soil could be regarded as undrained because of this characteristic. Thus, the test used an undrained shear. According to the frequency range of the seismic loading, the vibration frequencies adopted are f (1; 2; 4) Hz; the ratio of the dynamic stress amplitude σd to the double confining pressure σ_c is defined as the dynamic stress ratio r, (Equation (1)).

$$r = \sigma_d/2\sigma_c \tag{1}$$

The experimental dynamic stress ratios are r (0.165; 0.25; 0.335). The dynamic triaxial tests of consolidation ratio K_c (1; 1.25; 1.5) were performed to consider the influence of the initial shear stress on the dynamic characteristics of the saturated clay, in Equation (2).

$$K_c = (\sigma_s+\sigma_c)/\sigma_c, \tag{1}$$

where σ_s represents the initial shear stress, σ_c represents the consolidation confining pressure, and the magnitude of K_c reflects the initial shear stress level of the soil.

Given the asymmetry and irregularity of the seismic loading, repeating the earthquake with the same seismic waveform is impossible. Therefore, the seismic loading input in this study was simulated by a sine wave of equal amplitude waveform. The specific test plan is shown in **Table 2**.

Table 2: Saturated clay dynamic triaxial test program

Test type	Consolidation ratio K_c	Confining pressure (kPa)	Vibration frequency (Hz)	Dynamic stress ratio r
Isobaric pressure	1	50 100 150	1 2 4	0.165 0.25 0.335
Unsymmetrical pressure	1.25 1.5	50 100 150	4	0.165 0.25 0.335

3 DETERMINATION OF THE DYNAMIC STRENGTH FAILURE CRITERION OF THE SATURATED CLAY

3.1 Dynamic strength failure criterion of saturated clay

For saturated clay, hysteresis exists in the pore-water pressure test because of the poor drainage conditions inside the soil. Thus, the strain failure criterion is usually selected. Two ways are normally used to achieve the failure criterion of the soil strain. One way is to select a large dynamic stress and reduce the number of cycles; the other is to select a small dynamic stress and increase the number of cycles. For the selection of the strain failure criterion, the axial strain ε_p is usually specified as a certain value, and the commonly used strain failure criteria are ε_p (2.5; 5; 10) %. In this study the strain value ε_{tp} corresponding to the turning point is concentrated in the range 1–3 % by analysing the data of the strain-development curve above. Therefore, three conditions, ε_p (2.5; 5) % and $\varepsilon_p = \varepsilon_{tp}$, were chosen to study the dynamic-strength failure criterion of the saturated clay in this study. The differences in the dynamic strength of the saturated clay under three failure criteria were quantitatively analysed by selecting the appropriate failure criterion from the experimental data.

3.2 Dynamic strength curve of saturated clay

A soil's dynamic strength is expressed as the relationship between the number of cyclic vibration N and the dynamic stress σ_d when the failure criterion is reached, i.e., the $\sigma_d - N$ curve, also called the soil dynamic strength curve. Two dynamic strength parameters, namely, the dynamic cohesion c_d and the dynamic internal friction angle φ_d, can be obtained from the soil's dynamic strength curves through a set of soil dynamic strength tests. The specific solution process is as follows.

According to the soil dynamic strength, i.e., the $\sigma_d - N$ curve, obtained by the cyclic loading test, the dynamic stress amplitude σ_d required to reach the specified strain failure criterion under a certain fixed vibration times N can be determined under this state with pre-pressure. The following treatments are also needed to obtain the soil's dynamic strength parameters, namely, the dynamic cohesion c_d and the dynamic internal friction angle φ_d, under the test conditions. σ_1 and σ_3 are known, and $\sigma_1 = \sigma_3$ are under equal pressure consolidation conditions. The principal stress $\sigma_{1d} = \sigma_1 + \sigma_d$ and $\sigma_{3d} = \sigma_3$ of the dynamic failure condition can be obtained by determining the dynamic strength σ_d corresponding to the strain-failure criterion under the specified vibration times in the dynamic strength curves. From this approach, the molar stress circle under the dynamic failure condition can be drawn in the τ-σ coordinate map. A set of molar stress circles can be obtained by dynamic triaxial tests on a set of different confining pressures. The soil's dynamic strength parameters, namely, the dynamic cohesion c_d

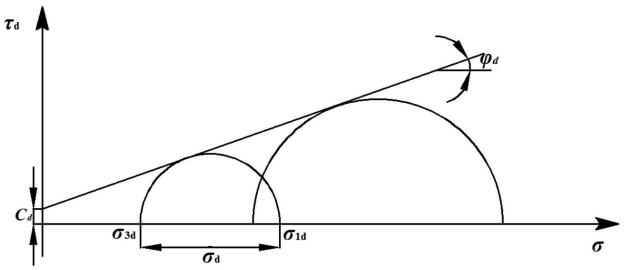

Figure 1: Soil dynamic strength and molar stress circle

and the dynamic internal friction angle φ_d, can be obtained by solving the intercept and the slope of the common tangent of the set of molar stress circles, as shown in **Figure 1**.

3.3 Effects of strain failure criterion on the dynamic strength of saturated clay

The definition of the soil's dynamic strength indicates that dynamic strength is closely related to the strain-failure criterion. The selection of the appropriate strain failure criterion is related to whether the soil damage conditions can be truly reflected. **Figure 2** shows the dynamic strength curve of the saturated clay when the confining pressure is 100 kPa, the vibration frequency is 4 Hz, the consolidation ratio is 1, and the strain failure criteria are ε_{tp}, 2.5 % and 5 %.

Figure 2 also shows that as the number of cyclic vibrations increases, the dynamic strength of the soil gradually decreases. In addition, an inflexion point exists in the dynamic strength curve. The relationship curve is steep before the inflexion point, i.e., the tangent slope is high when the number of vibrations is low. This finding indicates that the dynamic strength of the soil decays quickly. The relationship curve is gradually gentle after the inflexion point, i.e., the tangent slope of the relationship curve gradually decreases as the number of vibrations increases. This observation indicates that the dynamic strength decay tends to be slow.

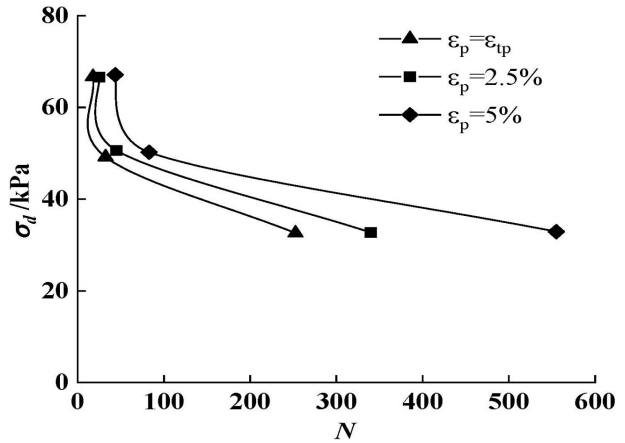

Figure 2: Dynamic strength curves of soil under different strain-failure criteria

Figure 2 further shows that the strain-failure criterion has a considerable influence on the dynamic strength analysis of the soil, and the improvement of the strain-failure criterion artificially increases the soil's dynamic strength. Under the same dynamic stress conditions, the higher the strain failure criterion is, the higher the required number of vibration times is for the soil to reach the break. Under the same vibration times, the higher the strain failure criterion is, the greater the required dynamic stress is for the soil to reach the break. **Figure 2** shows that the curves of the dynamic strength-vibration times of the soil corresponding to ε_p = 2.5 % and $\varepsilon_p = \varepsilon_{tp}$ are relatively close. This finding indicates that the strain-failure criterion ε_p = 2.5 % and $\varepsilon_p = \varepsilon_{tp}$ can be used to reflect the soil-damage situation realistically and evaluate the soil's dynamic strength objectively. However, the strain-failure criterion ε_p = 5 % does not usually reflect the true damage to the soil, and it overestimates the soil's dynamic strength. The higher the number of vibrations is, the more obvious this phenomenon is.

3.4 Determination of the strain-failure criterion

A soil's dynamic strength is inextricably linked to the number of cyclic vibrations. Thus, the concept of equivalent failure vibration times is introduced to analysing the 's dynamic strength under seismic loading. The waveforms used for cyclic loading in the dynamic triaxial test often have certain regularity, such as the equal-amplitude sinusoidal waveform used in this study, which is different to the vibration waveform caused by seismic loading in the actual situation. According to the "Foundation Dynamic Characteristics Test Specification", the equivalent failure vibration times N_f must be used in replacing the vibration times of the cyclic loading in the test process when the soil's dynamic strength is analysed to reduce the difference in the effects of the two kinds of loading on the soil. Moreover, the equivalent failure vibration times is related to the magnitude. The correspondence is shown in **Table 3**.

Table 3: Correspondence of earthquake magnitude–equivalent failure vibration times

Earthquake magnitude *M*	6.0	6.5	7.0	7.5	8.0
Equivalent failure vibration times N_f	5	8	12	15–20	26–30

3.5 Strain-failure criterion of saturated clay under earthquake loading

The analysis in the previous section indicates that the differences in the strain-failure criteria have an important influence on the soil's dynamic strength. In this section, quantitative research on the dynamic strength parameters of saturated clay under different strain-failure criteria is performed to illustrate the importance of selecting an appropriate strain-failure criterion. The curves of dynamic

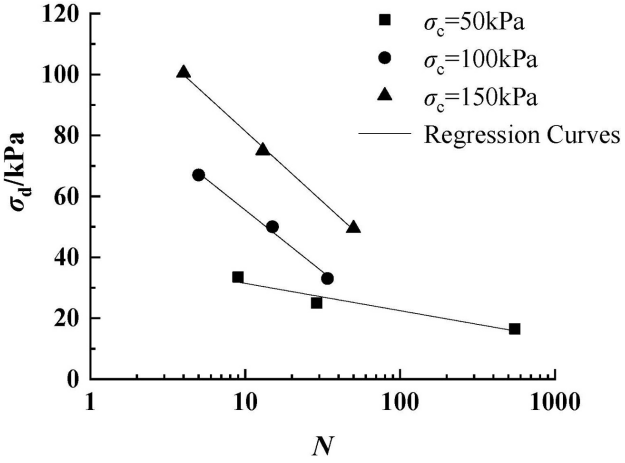

Figure 3: Dynamic strength curves of saturated clay at ε_p = 2.5 %

strength–vibration times of the soil corresponding to $\varepsilon_p = \varepsilon_{tp}$ and ε_p = 2.5 % are relatively close at the low vibration times. Thus, given the wide range of vibration times, the dynamic strength parameters of the soil are analysed in this study by selecting ε_p = 2.5 % and $\varepsilon_p = \varepsilon_{tp}$.

Figure 3 shows the dynamic strength curves of the strain-failure criterion ε_p = 2.5 % of saturated clay when the consolidation ratio is 1, the vibration frequency is 1 Hz, and the confining pressures are (50; 100; 150) kPa. The dynamic strength curve approximates a straight line in the logarithmic coordinate, i.e., the relationship between the dynamic stress and the vibration times in the logarithmic coordinate is linear. Therefore, the expression of the dynamic stress–vibration times is assumed as follows (Equation (3)):

$$\sigma_d = a \ln(N) + b \tag{3}$$

where a and b are the constants associated with the test conditions. The following are obtained by fitting the dynamic strength curves under different confining pressures in **Figure 3**:

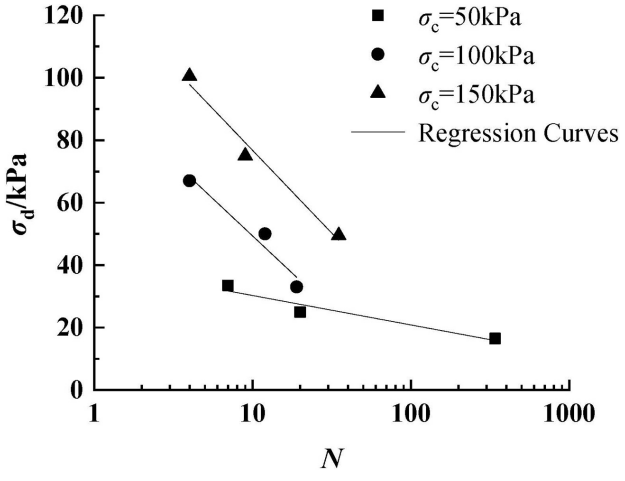

Figure 4: Saturated-clay dynamic strength curves at $\varepsilon_p = \varepsilon_{tp}$

$$\sigma_c = 50 \text{ kPa}, \sigma_d = -3.89 \ln N + 40.40 \tag{4}$$

$$\sigma_c = 100 \text{ kPa}, \sigma_d = -17.61 \ln N + 96.05 \tag{5}$$

$$\sigma_c = 150 \text{ kPa}, \sigma_d = -20.16 \ln N + 127.85 \tag{6}$$

Then, the dynamic stress required for the equivalent failure vibration times corresponding to different earthquake magnitudes is calculated. The dynamic cohesion c_d and dynamic internal friction angle φ_d of the soil under different equivalent failure vibration times are also calculated. The results of the calculation are shown in **Table 4**.

Table 4: Dynamic strength parameters of soil under equivalent failure vibration times at ε_p = 2.5 %

Equivalent failure vibration times N_f	Total stress (kPa)	Consolidation confining pressure (kPa)	Dynamic stress (kPa)	Dynamic cohesion (kPa)	Dynamic internal friction angle (°)
5	87.68	50	37.68	11.08	12.62
	183.74	100	83.74		
	263.76	150	113.76		
8	86.87	50	36.87	10.97	12.49
	180.15	100	80.15		
	259.64	150	109. 64		
12	86.20	50	36.20	10.24	12.08
	177.05	100	77.05		
	256.09	150	106.09		
20	85.34	50	35.34	9.56	11.68
	173.14	100	73.14		
	251.62	150	101.62		
26	84.89	50	34.89	8.99	11.61
	171.14	100	71.14		
	249.32	150	99.32		

Figure 4 shows the dynamic strength curves of the strain-failure criterion $\varepsilon_p = \varepsilon_{tp}$ of saturated clay when the consolidation ratio is 1, the vibration frequency is 1 Hz, and the confining pressures are (50; 100; 150) kPa. The dynamic stress is assumed to be linear with the number of vibrations in logarithmic coordinates.

The following are obtained by fitting the dynamic strength curves under different confining pressures in **Figure 4**:

$$\sigma_c = 50 \text{ kPa}, \sigma_d = -4.09 \ln N + 39.68 \tag{7}$$

$$\sigma_c = 100 \text{ kPa}, \sigma_d = -20.66 \ln N + 96.94 \tag{8}$$

$$\sigma_c = 150 \text{ kPa}, \sigma_d = -23.02 \ln N + 129.79 \tag{9}$$

The dynamic cohesion c_d and the dynamic internal friction angle φ_d of the soil under different equivalent failure vibration times when $\varepsilon_p = \varepsilon_{tp}$ are calculated, and the calculation results are shown in **Table 5**.

Table 5: Dynamic strength parameters of soil under different equivalent failure vibration times at $\varepsilon_p = \varepsilon_{tp}$

Equivalent failure vibration times N_f	Total stress (kPa)	Consolidation confining pressure (kPa)	Dynamic stress (kPa)	Dynamic cohesion (kPa)	Dynamic internal friction angle (°)
5	86.82	50	36.82	10.86	12.56
	182.50	100	82.50		
	263.70	150	113.70		
8	85.99	50	35.99	10.48	12.26
	178.28	100	78.28		
	258.20	150	108.20		
12	85.27	50	35.27	9.72	12.01
	174.64	100	74.64		
	254.31	150	104.31		
20	84.36	50	34.36	9.04	11.59
	170.06	100	70.06		
	249.41	150	99.41		
26	83.89	50	33.89	8.65	11.42
	167.71	100	67.71		
	246.90	150	96.90		

Figure 5 shows the relationship curves between the dynamic strength parameters c_d and φ_d of the saturated clay and the equivalent failure vibration times N_f when $\varepsilon_p = \varepsilon_{tp}$ and $\varepsilon_p = 2.5$ %.

Figure 5 shows that the corresponding relationship curves of c_d–N_f and φ_d–N_f are relatively close when the strain-failure criteria are $\varepsilon_p = \varepsilon_{tp}$ and $\varepsilon_p = 2.5$ %, respectively. This observation can prove that the calculated values of the soil's dynamic strength parameters c_d and φ_d when the strain-failure criteria are $\varepsilon_p = \varepsilon_{tp}$ and $\varepsilon_p = 2.5$ %, respectively, are slightly different. In addition, the value of the transitional strain ε_{tp} has a certain uncertainty. Thus, $\varepsilon_p = 2.5$ % can be used to replace $\varepsilon_p = \varepsilon_{tp}$ when the dynamic strength parameters of the saturated clay are calculated under the equivalent failure vibration times of the seismic loading.

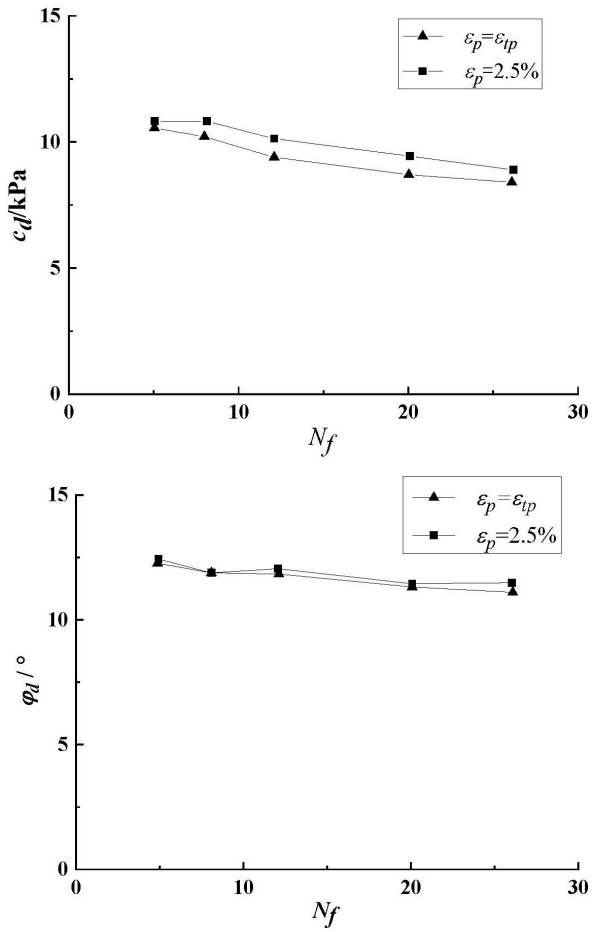

Figure 5: Relationship curves of c_d–N_f and φ_d–N_f under different failure criteria

4 TEST RESULTS AND ANALYSIS

4.1 Effects of initial shear stress on the dynamic strength characteristics of saturated clay

Figure 6 shows the dynamic strength curves of the saturated clay when the soil's strain-failure criterion is 2.5 %, the confining pressure is 100 kPa, the vibration frequency is 4 Hz, and the consolidation ratios are 1, 1.25 and 1.5. **Figure 6** shows that the initial shear stress has a considerable influence on the dynamic strength of the saturated clay. For the same dynamic stress, the larger the initial shear stress is, the less the required vibration time is for the soil to meet the strain-failure criterion, and the lower the dynamic strength of the soil is. Under the same vibration times, the greater the initial shear stress is, the smaller the required dynamic stress is for the soil to meet the strain failure criterion. In particular, when the initial shear stress is small, it puts pre-pressure on the soil, thereby improving the dynamic strength of the soil; when the initial shear stress is large, the bond between the particles inside the clay is destroyed, thereby reducing the dynamic strength of clay. An inflexion point exists in the dynamic strength curve of the soil. The smaller the initial shear stress is, the

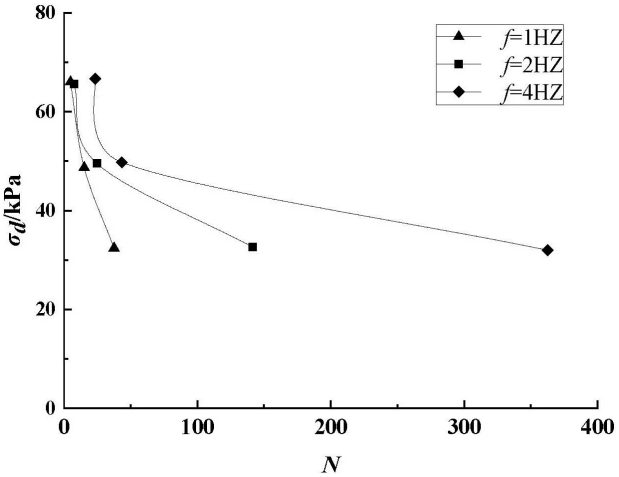

Figure 6: Dynamic strength curves of the saturated clay under different initial shear stresses

smoother the dynamic strength curve is after the inflexion point, and the smaller the tangent slope of the curve is.

4.2 Effects of initial shear stress on the dynamic strength parameters of saturated clay

The above analysis indicates that the initial shear stress has a considerable effect on the dynamic strength of saturated clay. In this section, the dynamic strength parameters of the saturated clay are quantitatively analysed to study the influence of the initial shear stress on the dynamic strength parameters.

Figure 7 shows the dynamic strength curves of the saturated clay when the consolidation ratio is 1, the vibration frequency is 4 Hz, the strain failure criterion is 2.5 %, and confining pressures are (50; 100; 150) kPa.

The dynamic strength curves under different confining pressures are analysed using Equation (1):

$$\sigma_c = 50 \text{ kPa}, \sigma_d = -3.71 \ln N + 39.68 \quad (10)$$

$$\sigma_c = 100 \text{ kPa}, \sigma_d = -12.40 \ln N + 103.63 \quad (11)$$

$$\sigma_c = 150 \text{ kPa}, \sigma_d = -18.36 \ln N + 142.82 \quad (12)$$

Then, the dynamic stress required for the equivalent failure vibration times corresponding to different earthquake magnitudes is calculated. The dynamic cohesion c_d and the dynamic internal friction angle φ_d of the soil under different equivalent failure vibration times are also calculated. The results of the calculation are shown in **Table 6**.

Table 6: Dynamic strength parameters of soil under different equivalent failure vibration times at $K_c = 1$

Equivalent failure vibration times N_f	Total stress (kPa)	Consolidation confining pressure (kPa)	Dynamic stress (kPa)	Dynamic cohesion (kPa)	Dynamic internal friction angle (°)
5	91.10	50	41.10	13.44	13.71
	194.94	100	94.94		
	279.99	150	129.99		
8	90.35	50	40.35	12.84	13.66
	192.41	100	92.41		
	276.35	150	126.35		
12	89.70	50	39.70	12.46	13.49
	190.23	100	90.23		
	273.09	150	123.09		
20	88.88	50	38.88	11.51	13.19
	187.48	100	87.48		
	269.00	150	119.00		
26	88.45	50	38.45	11.11	13.08
	186.06	100	86.06		
	266.89	150	116.89		

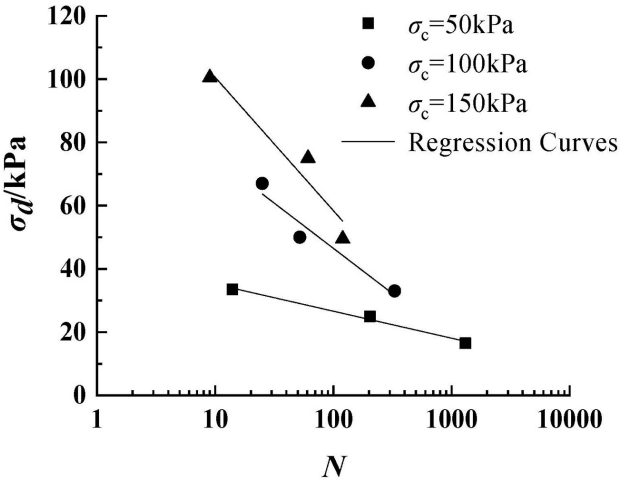

Figure 7: Dynamic strength curves of saturated clay at $K_c = 1$

Fi**gure 8** shows the dynamic strength curves of the saturated clay when the consolidation ratio is 1.25, the vibration frequency is 4 Hz, the strain failure criterion is 2.5 %, and the confining pressures are (50; 100; 150) kPa.

The dynamic strength curves under different confining pressures are analysed using Equation (1):

$$\sigma_c = 50 \text{ kPa}, \sigma_d = -4.49 \ln N + 43.46 \quad (13)$$

$$\sigma_c = 100 \text{ kPa}, \sigma_d = -11.87 \ln N + 97.03 \quad (14)$$

$$\sigma_c = 150 \text{ kPa}, \sigma_d = -17.08 \ln N + 132.89 \quad (15)$$

Then, the dynamic stress required for the equivalent failure vibration times corresponding to different earthquake magnitudes is calculated. The dynamic cohesion c_d and the dynamic internal friction angle φ_d of the soil under different equivalent failure vibration times are also calculated. The results of the calculation are shown in **Table 7**.

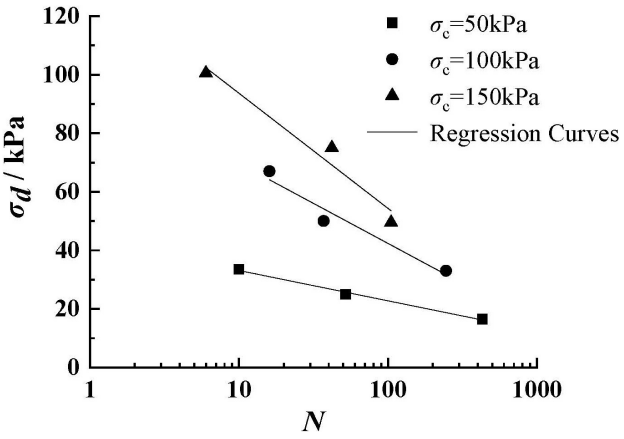

Figure 8: Dynamic strength curves of saturated clay at $K_c = 1.25$

Table 7: Dynamic strength parameters of soil under different equivalent failure vibration times at K_c = 1.25

Equivalent failure vibration times N_f	Total stress (kPa)	Consolidation confining pressure (kPa)	Dynamic stress (kPa)	Dynamic cohesion (kPa)	Dynamic internal friction angle (°)
5	90.32	50	40.32	11.94	13.37
	188.74	100	88.74		
	271.04	150	121.04		
8	89.41	50	39.41	11.53	12.94
	186.31	100	86.31		
	267.55	150	117.55		
12	88.62	50	38.62	11.28	12.77
	184.22	100	84.22		
	264.54	150	114.54		
20	87.62	50	37.62	10.74	12.52
	181.59	100	81.59		
	260.75	150	110.75		
26	87.11	50	37.11	10.15	12.48
	180.24	100	80.24		
	258.81	150	108.81		

Table 8: Dynamic strength parameters of soil under different equivalent failure vibration times at K_c = 1.5

Equivalent failure vibration times N_f	Total stress (kPa)	Consolidation confining pressure (kPa)	Dynamic stress (kPa)	Dynamic cohesion (kPa)	Dynamic internal friction angle (°)
5	89.87	50	39.87	11.08	13.19
	186.67	100	86.67		
	267.26	150	117.26		
8	88.78	50	38.78	10.86	12.84
	183.71	100	83.71		
	263.34	150	113.34		
12	87.86	50	37.86	10.50	12.55
	181.15	100	81.15		
	259.97	150	109.97		
20	86.65	50	36.65	9.86	12.19
	177.93	100	77.93		
	255.71	150	105.71		
26	86.04	50	36.04	9.54	12.06
	176.28	100	76.28		
	253.53	150	103.53		

Figure 9 shows the dynamic strength curves of the saturated clay when the consolidation ratio is 1.5, the vibration frequency is 4 Hz, the strain failure criterion is 2.5 %, and confining pressures are (50; 100; 150) kPa.

The dynamic strength curves under different confining pressures are analysed using Equation (1):

$$\sigma_c = 50 \text{ kPa}, \quad \sigma_d = -5.36 \ln N + 43.62 \tag{16}$$

$$\sigma_c = 100 \text{ kPa}, \quad \sigma_d = -14.52 \ln N + 96.82 \tag{17}$$

$$\sigma_c = 150 \text{ kPa}, \quad \sigma_d = -19.18 \ln N + 130.67 \tag{18}$$

Then, the dynamic stress required for the equivalent failure vibration times corresponding to different earthquake magnitudes is calculated. The dynamic cohesion c_d and the dynamic internal friction angle φ_d of the soil under different equivalent failure vibration times are also calculated. The results of the calculation are shown in **Table 8**.

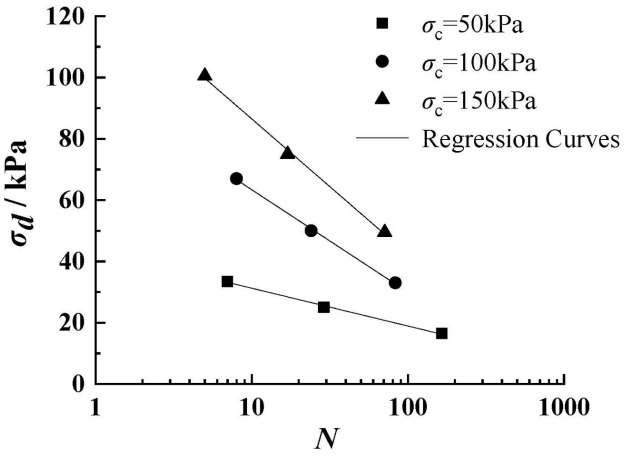

Figure 9: Dynamic strength curves of saturated clay at K_c = 1.5

Figure 10 shows the relationship curves between the dynamic strength parameters c_d and φ_d of the saturated clay and the equivalent failure vibration times N_f under different initial shear stresses.

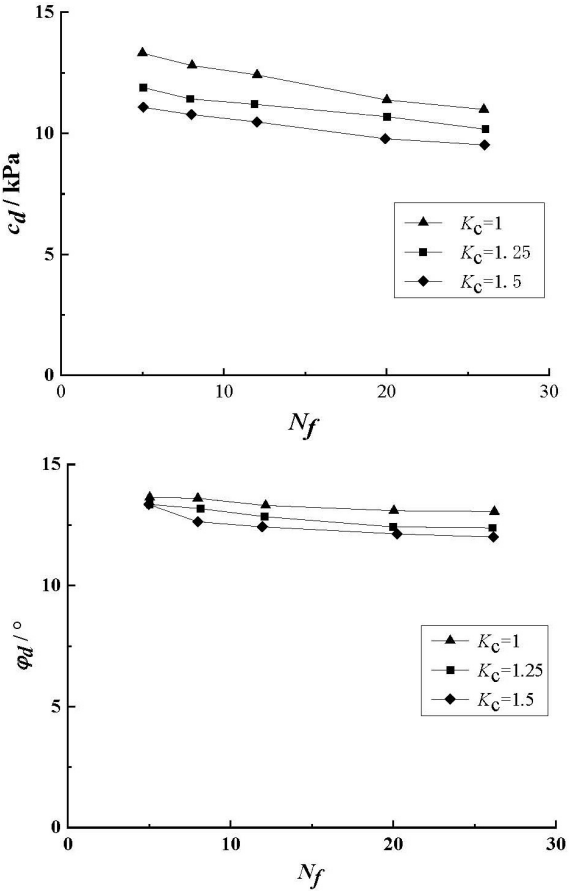

Figure 10: Relationship curves of c_d–N_f and φ_d–N_f of soil under different initial shear stresses

Figure 10 shows that the dynamic strength parameters of saturated clay are affected by the initial shear stress. The larger the initial shear stress is, the smaller the dynamic strength parameters of the soil are. This finding indicates that the existence of the initial shear stress reduces the soil's dynamic strength. Therefore, the effects of the initial shear stress on the saturated clay should be fully considered in the seismic design of engineering.

4.3 Effects of vibration frequency on the dynamic strength characteristics of saturated clay

Figure 11 shows the dynamic strength curves of the saturated clay when the strain-failure criterion is 2.5 %, the confining pressure is 100 kPa, the consolidation ratio is 1, and the vibration frequencies are (1; 2; 4) Hz.

Figure 11 shows that the vibration frequency influences the dynamic strength of the soil. Under the same dynamic stress, the higher the vibration frequency is, the higher the required vibration times is for the soil to reach the damage. This finding indicates that the soil's dynamic strength is large. Under the same vibration times, the higher the vibration frequency is, the greater the required dynamic stress is for the soil to reach the damage. In particular, the pore-water pressure has enough time to increase under the low-frequency cyclic loading, causing the soil sample to be destroyed in a small number of cycles. The pore-water pressure of the soft clay does not have enough time to increase under the high-frequency cyclic loading. According to the principle of effective stress, the higher the effective stress of the soil is, the higher the shear strength is. **Figure 11** also shows that after the inflexion point of the dynamic strength curve, the higher the vibration frequency is, the smoother the curve is, and the smaller the tangent slope of the curve is.

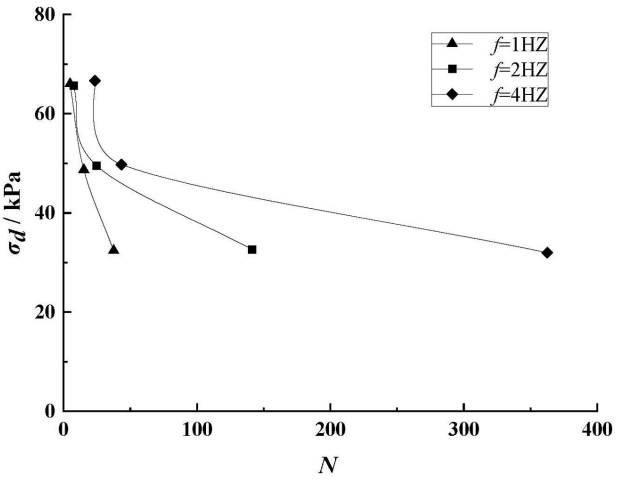

Figure 11: Dynamic strength curves of soil under different vibration frequencies at ε_p = 2.5 %

4.4 Effects of vibration frequency on the dynamic strength parameters of saturated clay

The above studies indicate that the dynamic strength of saturated clay is affected by the vibration frequency. The influence of vibration frequency on the dynamic strength parameters is studied by analysing quantitatively the equivalent failure dynamic strength parameters under seismic loading. **Figure 12** shows the dynamic strength curves of the saturated clay when the consolidation ratio is 1, the frequency is 2 Hz, the strain failure criterion is 2.5 %, and the confining pressures are (50; 100; 150) kPa.

The dynamic strength curves under different confining pressures are analysed using Equation (1):

$$\sigma_c = 50 \text{ kPa}, \sigma_d = -4.49 \ln N + 43.46 \quad (19)$$

$$\sigma_c = 100 \text{ kPa}, \sigma_d = -4.49 \ln N + 43.46 \quad (20)$$

$$\sigma_c = 150 \text{ kPa}, \sigma_d = -4.49 \ln N + 43.46 \quad (21)$$

Then, the dynamic stress required for the equivalent failure vibration times corresponding to different earthquake magnitudes is calculated. The dynamic cohesion c_d and the dynamic internal friction angle φ_d of the soil under different equivalent failure vibration times are also calculated. The calculation results are shown in **Table 9**.

Table 9: Dynamic strength parameters of soil under different equivalent failure vibration times at f = 2 Hz

Equivalent failure vibration times N_f	Total stress (kPa)	Consolidation confining pressure (kPa)	Dynamic stress (kPa)	Dynamic cohesion (kPa)	Dynamic internal friction angle (°)
5	89.01	50	39.01	12.69	13.19
	190.76	100	90.76		
	272.20	150	122.20		
8	88.27	50	38.27	12.27	12.86
	187.86	100	87.86		
	268.15	150	118.15		
12	87.63	50	37.63	11.41	12.78
	185.37	100	85.37		
	264.65	150	114.65		
20	86.83	50	36.83	10.70	12.55
	182.25	100	82.25		
	260.23	150	110.23		
26	86.42	50	36.42	9.82	12.52
	180.61	100	80.61		
	257.97	150	107.97		

Table 9 shows the equivalent failure dynamic strength parameters of saturated clay at the vibration frequency f = 2 Hz. **Table 6** shows the equivalent failure dynamic strength parameters of saturated clay at the vibration frequency f = 4 Hz.

Figure 13 shows the relationship curves between the dynamic strength parameters c_d and φ_d of saturated clay and the equivalent failure vibration times N_f at different vibration frequencies. **Figure 13** shows that the dynamic

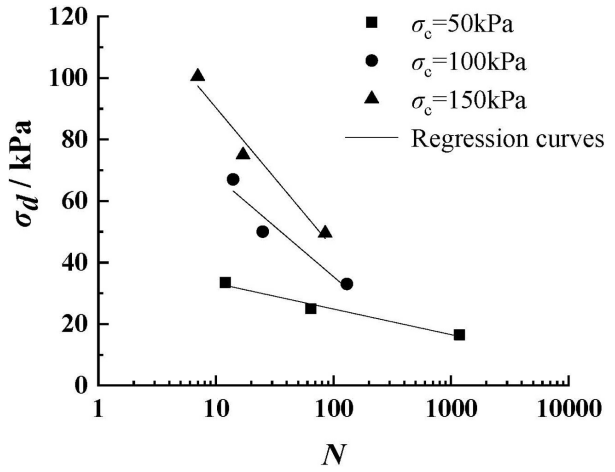

Figure 12: Dynamic strength curves of saturated clay at f = 2 Hz

strength parameter of the saturated clay is affected by the loading vibration frequency. The lower the vibration frequency is, the smaller the dynamic strength parameter of the soil is.

5 CONCLUSIONS

The dynamic strength characteristics of saturated clay in Wenchuan area were studied using a dynamic triaxial test system. Firstly, the influences of different strain-failure criteria were analysed based on the definition of soil dynamic strength, and the appropriate strain-failure criterion was determined based on the test data. Then, the dynamic strength parameters of the saturated clay in the Wenchuan earthquake area under seismic loading equivalent failure vibration times were calculated. Finally, the effects of the initial shear stress and the vibration frequency on the dynamic strength of the saturated clay were studied. The conclusions are as follows:

1. Qualitative and quantitative studies on the dynamic strength of the saturated clay under different strain-failure criteria indicate that selecting the strain-failure criterion with a strain value of 2.5 % and a transitional strain is objective for a soil dynamic strength evaluation. Moreover, $\varepsilon_p = \varepsilon_{tp}$ can be replaced by ε_p = 2.5 % when the dynamic strength parameter of the saturated clay under the seismic loading equivalent failure vibration times is calculated.
2. We conclude through the quantitative research on the dynamic strength parameters of the saturated clay that as the cyclic vibration time increases, the dynamic strength parameter of the soil gradually decreases. This finding indicates that the dynamic strength of the soil gradually decreases.
3. The dynamic strength parameters of the saturated clay in the Wenchuan earthquake area under different earthquake magnitudes are presented by introducing the equivalent failure vibration times of the soil under seismic loading.
4. The initial shear stress has a considerable effect on the dynamic strength of saturated clay. Under the same vibration times, the larger the initial shear stress is, the smaller the required dynamic stress is for the soil to break, and the smaller the dynamic strength parameter is. This finding indicates that the existence of the initial shear stress reduces the dynamic strength of the soil.
5. The vibration frequency has a considerable influence on the dynamic strength of saturated clay. Under the same vibration times, the higher the vibration frequency is, the greater the required dynamic stress is for the soil to break, and the greater the dynamic strength parameter is. This finding indicates that the soil dynamic strength is large.

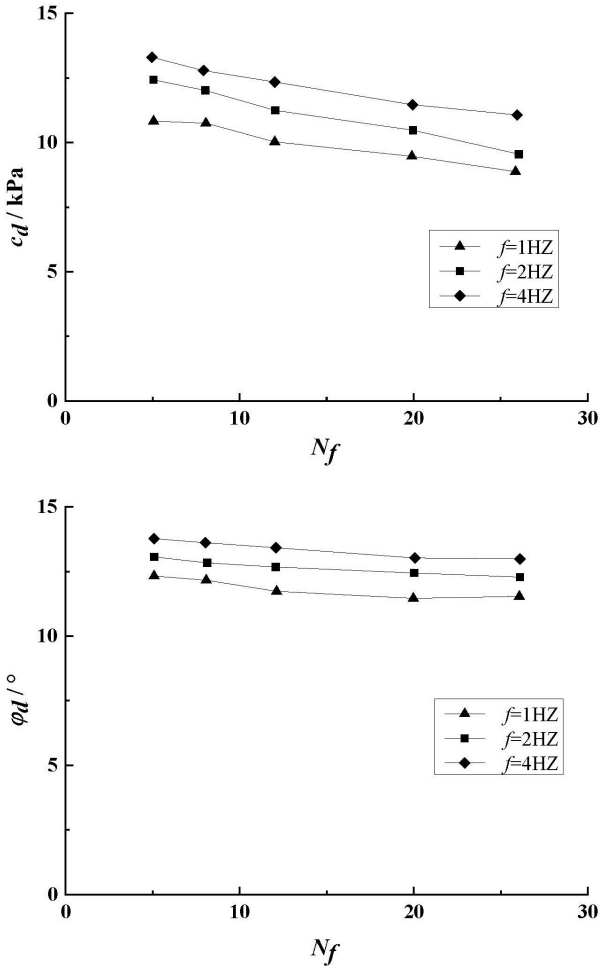

Figure 13: Relationship curves of c_d–N and φ_d–N of saturated clay under different vibration frequencies

Acknowledgments

The authors are grateful for sponsorship by the Qing Lan Project, the research project of the Ministry of Housing and Urban-Rural Development (No.

2019-K-131), the research project of the Nanjing Construction System Scientific (No.Ks2039), the research project of Nanjing Vocational Institute of Transport Technology (No. JZ2001).

6 REFERENCES

[1] K. Pan, Z. X. Yang, Effects of initial static shear on cyclic resistance and pore pressure generation of saturated sand, Acta Geotechnica, 13 (**2018**) 2, 473–487, doi:10.1007/s11440-017-0614-5

[2] Y. Feng, W. Zhang, Y. X. Ma, Experimental study on stress-water content-strain relationship of remolded loess under directional shear stress path, Journal of Qinghai University, 36 (**2018**) 1, 47–53

[3] Z. L. Zhou, G. X. Chen, Q. Wu, Effect of initial static shear stress on liquefaction and large deformation behaviors of saturated silt, Yantu Lixue/rock & Soil Mechanics, 38 (**2017**) 5, 1314–1320

[4] Z. X. Yang, K. Pan, Flow deformation and cyclic resistance of saturated loose sand considering initial static shear effect, Soil Dynamics & Earthquake Engineering, 92 (**2017**), 68–78, doi:10.1016/j.soildyn.2016.09.002

[5] Z. H. Zhang, X. C. Huang, Q. T. Bi, Effect of initial shear stress and phase difference on dynamic characteristics of saturated sand, Yangtze River, 48 (**2017**) 3, 70–74

[6] G. Suazo, A. Fourie, J. Doherty, Effects of confining stress, density and initial static shear stress on the cyclic shear response of fine-grained unclassified tailings, Geotechnique, 66 (**2016**) 5, 1–12, DOI:10.1680/jgeot.15.P.032

[7] J. Wang, P. Luo, F. Y. Liu, Effect of angle between directions of initial shear stress and cyclic load on softening properties of soft clay, Chinese Journal of Rock Mechanics and Engineering, 35 (**2016**) 5, 1072–1080

[8] J. T. Cao, Experimental study on dynamic behaviors of Wenchuan earthquake area saturated sand under cyclic loading, Nanjing, Hohai University, 2014

[9] T. Wichtmann, T. Triantafyllidis, Influence of the Grain-Size Distribution Curve of Quartz Sand on the Small Strain Shear Modulus Gmax, Journal of Geotechnical and Geoenvironmental Engineering, 35 (**2009**) 10, 1404–1418, doi:10.1061/(ASCE)GT.1943-5606.0000096

[10] Y. Yilmaz, M. Mollamahmutoglu, Characterization of Liquefaction Susceptibility of Sands by Means of Extreme Void Ratios and/or Void Ratio Range, Journal of Geotechnical and Geoenvironmental Engineering, 135 (**2009**) 12, 1986–1990, doi:10.1061/(ASCE)GT.1943-5606.0000164

[11] K. Yasuhara, Post-cyclic undrained strength for cohesive soils, Journal of Geotechnical Engineering, 120 (**1994**) 11, 1961–1979, doi:10.1061/(ASCE)0733-9410(1994)120:11(1961)

[12] I. Ishibashi, M. Kawamura, S. K. Bhatia, Effect of initial shear on cyclic behavior of sand, Journal of the Geotechnical Engineering, 119 (**1985**) 12, 1395–1412

[13] H. B. Seed, C. K. Chan, Clay strength under earth quake loading conditions, Journal of Soil Mechanics and Foundations, 92 (**1966**) 2, 53–78, doi:10.1061/JSFEAQ.0000867

[14] T. F. Zimmie, C. Y. Lien, Response of clay subjected to combined cyclic and initial static shear stress, Proc. 3rd Can. Conf. on Marine Geotech. Eng., 1986

[15] A. M. Goulois, R. V. Whitman, K. Hoeg, Effects of sustained shear stresses on the cyclic degradation of clay, Strength testing of marine sediments, ASTM STP 883, R. C. Chaney and K. R. Demars, eds. ASTM Philadelphia, 1985, doi:10.1520/STP36344S

[16] G. Lefebvre, P. Pfendler, Strain rate and preshear effects in cyclic resistance of soft clay, Journal of Geotechnical Engineering, 122 (**1996**) 1, 21–26, doi:10.1061/(ASCE)0733-9410(1996)122:1(21)

[17] K. Tan, M. Vucetic, Behavior of medium and low plasticity clays under cyclic simple shear conditions, Proc. 4 th Int. Conf. on Soil Dyn. and Earthquake Eng., A. S. Cakmak and I. Herra, eds. Mexico City, Mexico, 1989

[18] T. Matsui, H. Ohara, T. Ito, Cyclic stress strain history and shear characteristic of clays, Journal of Geotechnical Engineering, 106 (**1980**) 10, 1101–1120

[19] J. H. Liao, M. H. Yu, T. Akira, Dynamic shear strength of loessial soils and volcanic cohesive soils, Journal of Xi'an Jiaotong University, 32 (**1998**) 10, 70–74

[20] Y. M. Chen, X. M. Ji,B. Huang,Effect of cyclic loading frequency on undrained behaviors of undisturbed marine clay, China Ocean Engineering, 18 (**2004**) 4, 634–651